Dissolution Kinetics of Quartz and Granite in Acidic and Basic Salt Solutions

W. Gabriel Worley and Jefferson W. Tester

Energy Laboratory, Massachusetts Institute of Technology
77 Massachusetts Avenue, Room E40-455
Cambridge, Massachusetts 02139-4307

Key words: dissolution kinetics, rock-water interactions, hot *dry* rocks

ABSTRACT

Of importance to Hot Dry Rock (HDR) geothermal energy development is the characterization of the rate of dissolution of host reservoir rock as a function of temperature, pressure, and liquid phase composition. Experiments were carried out in a continuous-flow titanium spinning basket reactor from 100' to 200°C. Nitric acid solutions down to pH 1.1 showed very little effect on the quartz dissolution rate. The effect of hydroxide ion concentration and ionic strength were evaluated in pure NaOH, NaOH/NaCl, and $NaOH/Na_2SO_4$ solutions. The fractional order dependency of the quartz dissolution rate on hydroxide ion and sodium ion (or ionic strength) concentration were determined in NaOH/NaCl solutions. Quartz dissolution rates were slower in $NaOH/Na_2SO_4$ solutions than in NaOWNaCl solutions at sodium concentrations higher than 0.01 molal. The apparent activation energy from 100' to 200°C in deionized water to NaOWNaCl solutions up to 0.01 molal hydroxide ion and 0.1 molal sodium ion was estimated to be 83 (±5) kJ/mol. Granite dissolution experiments at 200°C were also performed to provide a more realistic model of typical reservoir rock found in HDR systems. The dissolution rate of albite and quartz in granite were estimated to be one to two orders of magnitude faster than individual dissolution rates.

1. INTRODUCTION

Rock-water interactions are important in a wide variety of geologic environments. Researchers have been motivated either because of their interest in understanding important natural geologic processes in the earth or because of a need to quantify dissolution rates for chemical processes above ground or for geothermal energy extraction underground using heat mining concepts. The motivation for carrying out this project was driven by engineering issues related to mineral transport in circulating hot dry rock (HDR) geothermal systems (Armstead and Tester, 1987; Charles *et al.*, 1979; Grigsby *et al.,* 1989; Tester *et al.*, 1977). Of critical importance to HDR is the characterization of the rate of dissolution of host reservoir rock as a function of temperature, pressure and liquid phase composition. In general, quartz is a major mineral component in HDR reservoirs in low permeability crystalline rock. Furthermore, quartz is highly reactive relative to other constituent minerals in aqueous environments at temperatures of interest to HDR geothermal energy extraction (Charles, 1979).

Tester *et al.* (1994) analyzed the available literature data on quartz dissolution rates in deionized water from 25° to 625°C. While this treatment provides a good correlation of dissolution rates from twelve different investigations, natural geothermal environments consist of widely varying solution compositions. Several studies have investigated the pH effect on the dissolution rate of quartz at temperatures from 25° to 90°C (Kamiya *et al.*, 1974; Wollast and Chou, 1986; Knauss and Wolery, 1988; Grigsby, 1989; Brady and Walther, 1990; House and Orr, 1992). These low temperature studies show a large increase in dissolution rate as the pH is raised above pH 6, while below pH 6, the dissolution rate is nearly independent of pH. Only a few experimental studies have indicated a significant increase in rate as pH **is** lowered below 3. (Kamiya *et al.,* 1974; Grigsby, 1989) Some of the experiments were conducted at constant ionic strengths, some controlled pH using variable ionic strength buffers, while others simply add acids or bases to adjust pH. Rigorous comparison of the data requires the knowledge of how electrolyte concentration affects quartz dissolution. Dove and Crerar (1990) performed quartz dissolution experiments in 0 to 0.15 molal (mol/kg H_2O) solutions of NaCl, KCl, LiCl, $MgCl_2$, and found that in all cases the presence of electrolyte increased the rate above the values measured in deionized water. However, the effect of electrolytes may be different when acids or bases are added to the solution. The effect of pH and ionic strength has been studied by Gratz and coworkers (1990,1993) using "negative crystal" etching experiments at 166°C and 211°C, however, this technique can only be carried out over a limited range of ionic strengths and dissolution rates.

The primary objective of this paper is to quantify the effects of pH and ionic strength on the dissolution rate of quartz. Specifically, the effect of adding acids, bases, and salts on the rate of quartz dissolution was studied. Three experimental groups were camed out: (1) the effects of HNO_3 and NaOH at temperatures from 100° to 200°C with no salt present, (2) the effects of NaOH at 150°C with NaCl added to maintain a constant sodium concentration (constant ionic strength), and (3) the effects of added NaCl and Na_2SO_4 with NaOH added to maintain a constant OH^- concentration.

Granitic rocks are very common in low-permeability HDR systems, therefore we would like to understand the granite-water system. A first step towards this understanding was achieved by studying the dissolution behavior of core slabs and rock cuttings from the Fenton Hill test wells (Tester *et al.*, 1977; Charles, 1978, 1979; Robinson, 1982). Core slab studies at 200' and 295°C by Charles (1978, 1979) suggested that quartz was the dominant phase for dissolution activity in the HDR environment, consequently, studies of pure quartz dissolution were also undertaken. As a check on the applicability of our empirical quartz dissolution models to dissolution of the quartz phase in granite, we performed two granite dissolution experiments at 200°C.

2. METHODS

2.1 Experimental

The quartz dissolution rate experiments used Ottawa sand particles sieved to 595 to 850 μm, while the granite experiments used crushed granite sieved to 0.85 to 2.38 mm. The granite was a core sample from well EE-3A at Fenton Hill, New Mexico composed of four major mineral phases, as shown in Table 1. A commercially pure titanium spinning basket autoclave reactor (see Worley and Tester (1995a) for a complete description) was used to collect dissolution kinetics data, which approximates an ideal continuous-flow stirred tank reactor (CSTR). Mineral samples are pretreated in the reactor with deionized water at 150' to 200°C until the dissolution rate drops off to a constant value over time. Dissolution rates are calculated from the dissolved species in solution and the solution flow rate through the reactor (see Tester *et al.* (1994) for details). Aqueous silica or silicic acid concentration was measured using the molybdate blue method following the ASTM standard technique #D859. Inductively coupled plasma (ICP) emission spectroscopy was used to cross-

check the molybdate technique to ensure that silica polymerization was not significantly affecting the determination of dissolved SiO_2. ICP was also used in the analysis of the granite dissolution experiments to determine concentrations of Si. Al. Na. K. Ca. Mg. and Fe.

2.2 Rate Determination

Rate constants (k_f) determined from the ram experimental data are transformed into rate constant data using Equation (7a) from Tester *et al.* (1994):

$$k_f = \frac{r_{net}}{\frac{A_S}{M_W}\left(1 - m_{H_4SiO_4}/m^{sat}_{H_4SiO_4}\right)} \quad (1)$$

The mass of mater. M_W. is calculated as the product of the reactor liquid volume and the density of the water at reaction conditions. The total quartz surface area. A_S is calculated hy multiplying the specific surface area. a_S. by the mass of quartz used. M_{qtz}. **A** geometric surface area basis is used in this paper and discussed in Tester *rr al.* (1994). The net dissolution rate. r_{net}. is calculated differently depending on which reactor was used. For the spinning basket reactor. the CSTR assumption allows r_{net} to he calculated directly from the outlet concentration and the flow rate (see Tester *et al.* (1991) for details).

2.3 Correlation of Kinetic Data

The hasic hypothesis assumed is that H^+ and OH- catalyze the dissolution rate by some mechanism of interaction nith the quartz surface. In the previous work performed at low temperatures. rate data are typically reported as the logarithm of the rate versus pH. There are two potential complications with this approach. First. when correlating data over a range of temperatures at high pH. changes in the dissociation constant of water affect the apparent activation energy (see Section 3.5 for details). Second. the concentration of H^+ and OH- may he the appropriate regression parameter. rather than the activity. This issue is very difficult to resolve experimentally since dissolution rates can increase rapidly with changes in solution composition. while the activity coefficients may only change slightly. For this case. since activities and concentrations vary similarly. the quality of the regressions will be comparable regardless of which basis is used.

The concentration of ions in solution must be calculated at the reaction temperature in order for correlations to be meaningful. Based on the quantities of acid. base. and/or salt added to the feed tank at room temperature. a model was developed to calculate the ion concentration in the reactor. This model uses an iterative procedure to solve the equilibrium relations and the charge balance. incorporating experimental dissociation constants published in literature with activity coefficients calculated from the Extended Debye-Hückel equation (Zemaitis *et al.*, 1986). For a complete description of the model. see Worley and Tester (1995a).

Now that we have determined the dissolution rate and the concentration of ions in the reactor, all that is left is to develop a functional relationship between quantities. While the exact functional form of the relationship between the dissolution rate and the concentration of ions in solution is not known. empirical relations can be used to fit the data. Care must be taken not to assign too much mechanistic information from the results of the correlation. since results may change as more data are available.

Experiments at low pH show little effect on dissolution rate. and are therefore difficult to model in an experimentally significant manner. As a first approximation. the rate data in neutral and basic solutions can he represented with a simple global rate law of the following form:

$$k_f = k_{OH.Na}\, m^{b}_{OH^-}\, m^{c}_{Na^+} \quad (2)$$

where k_f is the global dissolution rate constant. m_{OH^-} and m_{Na^+} are molalities of OH- and Na^+. b and c are the apparent reaction orders of OH- and Na^+. respectively. and $k_{OH.Na}$ is an empirical rate constant with the dependencies on m_{OH^-} and m_{Na^+} factored out of k_f. Parameters regressed from experimental data using this equation are only valid for the system studied. For example. parameters regressed from a NaOH/NaCl mixture will not necessarily be equal to the regressed parameters from a NaOH/Na_2SO_4 mixture.

Although the form of the rate law in Equation (2) initially came from elementary reaction modeling where b and c are integers and represent the stoichiometries of the reactants involved in the activated complex. equations like Equation (2) have been used frequently to model complex kinetics where b and c are fitted to the experimental data and are no longer constrained to he integers. In this context. b and c are simply fitted parameters conveying little on no mechanistic information. However. in many situations. Equation (2) can fit rate data over a wide range of experimental parameters. and is thus a useful empirical tool.

Table 1. Modal Analysis of Fenton Hill Granodiorite.

Mineral	Formula	Volume %
Quartz	SiO_2	28.7%
Plagioclase	$NaAlSi_3O_8$ (Ah). $CaAl_2Si_2O_8$ (An) (72% Ah. 28% An)	*39.84*
Microcline	$KAlSi_3O_8$	16.8%
Biotite	$K(Mg,Fe^{+2})_3(Al,Fe^{+3})\,Si_3O_{10}$	9.2%
Minor Phases		5.5%

3. RESULTS

The following four sections describe the dissolution experiments carried out in order to quantiiy the effects of adding different electrolytes to the quartz-water system.

3.1 Effect of H^+ with no salt present

A set of experiments were carried out in the spinning basket reactor at 175°C and 200°C. Figure 1 displays the results of these experiments on a lop k_f versus pH (at 23°C) graph. The pH at the reaction temperature would be a more appropriate abscissa. however. the pH of HNO_3 solutions changes very little with temperature. because it is a strong acid (~100% dissociated) and the mean ionic activity coefficient. $\gamma_{\pm}(HNO_3)$. does not change much with temperature. The data at 175°C show a decreasing trend in k_f as pH is lowered from pH 4 to pH 3. **A** relatively pH independent region exists from pH 3 to pH 1.5. At pH 1.1. the dissolution rate begins to increase at 175°C. At *200°C.* the data show a decreasing trend from pH 4 down to pH *2.3.* The qualitative behavior at 175° and 200°C is consistent with the previous work performed at lower temperalures (Kamiya *et al.*. 1971: Wollast and Chou. 1986: Knauss and Wolery. 1988: Grigsby, 1989: Brady and Walther. 1990: House and Orr. 1992).

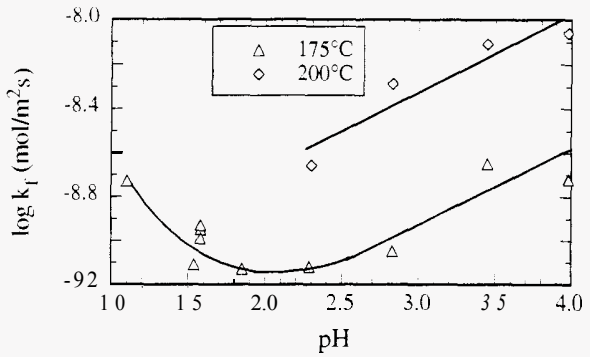

Figure 1. Quartz dissolution results in low pH solutions of HNO_3 at 175°C and 200°C. Lines drawn to illustrate trends only.

3.2 Effect of OH- (using NaOH)

All experiments investigating the effect of OH- on the dissolution rate of Ottawa sand in NaOH solutions are plotted in Figure *2*. A remarkably linear fit to the data is ohtainrd by plotting the logarithm of the dissolution rate constant. k_f. versus the logarithm of the hydroxide ion concentration (estimated using the speciation model discussed in Section *2.3)*. The hydroxide ion concentrations in Figure 2 are derived from deionized water to 0.01 molal SaOH solutions.

The slopes or apparent reaction orders on hydroxide ion. shown in Figure *2*. varied from 0.72 (±0.14) at 100°C to 0.88 (±0.04) at 200°C (Please note that all ± ranges given are at 95% confidence limits). Thus an empirical equation of the form:

$$k_f = k_{OH}\, m_{OH^-}^{b'}$$

is adequate to describe quartz dissolution rate data in SaOH solutions. where k_{OH} is an empirical dissolution rate constant and b' is the apparent reaction order on OH- with the effect of Na+ emhedded in it. All of the data plotted in Figure 2 are included in the regressions except for two points (one deionized water run and one run at log m_{OH^-} = -4.8) at 200°C that are clearly outliers (shown as filled in diamonds), lying 0.6 log units below the regressed line. These omitted runs (126 and 127) were performed sequentially: but no explanation can he given for their wide deviation from the other data at 200°C.

Equation (3) incorporates the effect of Sa+ into the value of 6'. Thus. we would like to decouple the effects of Na+ from the effects of OH-. A multivariate linear regression of these data using Equation *(2)* would result in inaccurate values of b and c. Therefore, experiments were carried out at constant Na+ (using NaCl) and variable OH-. and at constant OH- and variable Na^+. to more accurately determine the values of b and c in Equation *(2)*.

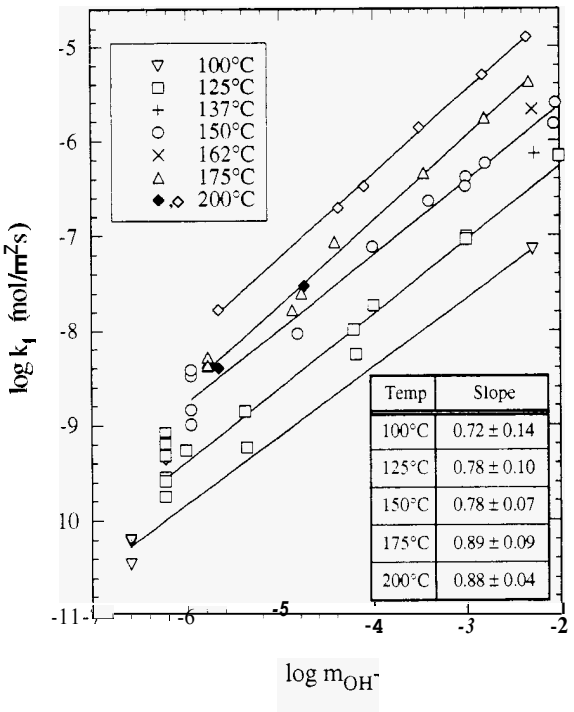

Figure 2. Quartz dissolution: The effect of added NaOH with no salts present. Two-parameter linear regression results shown (95% confidence). Note that two outlier points (◆) at 200°C were omitted from the regression and the average of the deionized water runs was used in the regression.

3.3 Effect of OH- at constant Na+

Experiments were performed at 150°C investigating the effect ot OH- on the dissolution rate of quartz at a constant Na^+ (0.01 molal) to decouple the effect of OH- from the effect of Na^+ in solution. Solutions varied from deionized water with NaCl added to 0.01 molal SaOH solution. The results are plotted in Figure 3 using log log $[k_f/(m_{Na^+})^c]$ versus lop m_{OH^-} coordinates to account for any variation in Na+ between experiments and to allow calculation of b in Equation (2) by a simple linear regression where the goodness of fit can be easily seen on a graph. The value of c is arbitrary. however. since m_{Na^+} is approximately constant. identical results were obtained for c = 0.2 to 0.4. Figure 3 shows that b = 0.58 (±0.17) assuming c = 0.3.

Although these results are only strictly valid for 150°C and m_{Na^+} = 0.01 molal, the studies shown in Figure *2* suggest that the combined effect of Na+ and OH- does not change measurably from deionized water to 0.01 molal NaOH solutions. Therefore, b and c are not expected to be strongly concentration dependent in the range of concentrations shown in Figure *2* (up to 0.01 molal). The value of 6 may change with temperature since the slopes in Figure *2* appear to be slightly temperature dependent.

3.4 Effect of Na^+ at constant OH'

The results of the experiments investigating the effect of Na+ ranging from $1x10^{-3}$ to 1.25 molal on k_f at 150°C with a OH^- concentration of approximately 10^{-3} molal in NaOH/NaCl solutions are shown in Figure 3 using Equation *(2)* as the basis for the correlation. Linear regressions on a log $[k_f/(m_{OH^-})^b]$ versus log m_{Na^+} result in a slope of 0.25 (±0.10) for b = 0.58. Identical results are obtained for b = 0.48 to 0.68. Clearly. the assumed value of 6 is not critical in the analysis of rate data at approximately constant m_{OH^-}. The effect of Na+ appears to be leveling off above log m_{Na^+} = -0.9 (m_{Na^+} = 0.13 molal). The slope of the regression neglecting the two high m_{Na^+} points is 0.31 (±0.06).

Experiments were also performed using Na_2SO_4 to vary the Na+ concentration instead of NaCl to investigate for the possible effects of the chloride anion. Results of these experiments are shown in Figure 3. The log m_{Na^+} = -2.0 point agrees well with the NaCl point at the same concentration. However. further increases in Na^+ concentration do not result in an experimentally significant increase in the rate. It appears that, at the same molal concentration. NaCl accelerates dissolution more than Na_2SO_4. This could imply an enhancing effect of Cl^- and/or an inhibiting effect of SO_4^{--} (or HSO_4^-). Perhaps SO_4^{--} adsorbs on the quartz surface limiting the effectiveness of attack by OH- and Na^+. The effect of the anion is expected to be small, since at these concentrations of OH- the quartz surface is negatively charged.

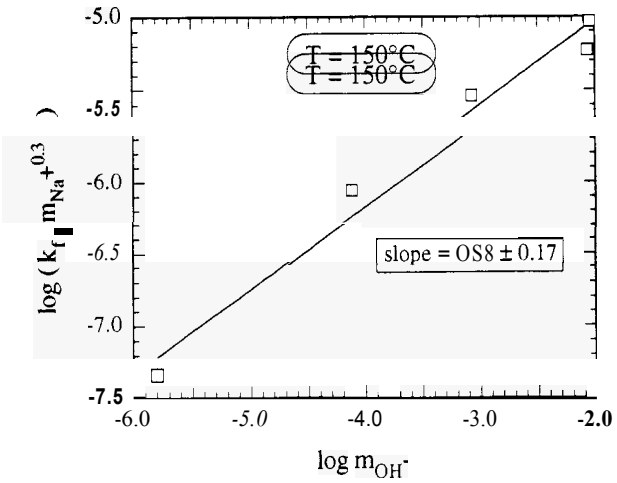

Figure 3. Quartz dissolution results showing the effect of OH- at constant Na+ (–0.01 molal). Two-parameter linear regression given with 95% confidence interval in slope.

which should hinder the adsorption of the negatively charged anion.

Despite the differences between the NaCl and Na_2SO_4 experimental results, both data sets display a leveling off of the Na+ enhancement effect. This behavior is consistent with a saturation of the quartz surface.

3.5 Regression Analysis of Dissolution Rate Data

The individual regression analyses in Sections 3.3 and 3.4 could have been replaced by a single multivariate analyses, however simple graphs like Figures 3 and 4 could not have been drawn to visually validate the goodness of fit. In this section, a multivariate analyses is employed to estimate the parameters in Equation (2), using the NaOH/NaCl data in the present study at 150°C. The two high m_{Na^+} runs were excluded from the analysis, since these data showed that the dissolution rate levels off as m_{Na^+} is increased and the global kinetic model given in Equation **(2)** cannot predict this behavior.

Equation **(2)** was useful in fitting most of our rate data, however, it cannot be used to estimate the dissolution rates in deionized water. Since Figure 2 showed that the experiments in NaOH solutions only extrapolated well to the deionized water data, we would like to derive a relationship that can describe all of our data in deionized water and NaOH/NaCl solutions using one simple equation. The following equation was found to be effective in correlating our rate data:

$$k_f = k_{OH,I}\, m_{OH^-}^{b}\, I^{c} \qquad (4)$$

where **I** is the ionic strength of the solution in units of molality and $k_{OH,I}$ is the empirical rate constant used to factor out the dependencies on m_{OH^-} and I from k_f. The ionic strength is calculated using the following expression:

$$\mathrm{I} = \frac{1}{2}\sum_i z_i^2 m_i \qquad (5)$$

where z_i and m_i are the ionic charge and molality (mol/kg H20) of ionic species i, respectively. The value of **I** is essentially equivalent to m_{Na^+} for all solutions except for the deionized water runs where it is equivalent to m_{H^+}. The choice of **I** was used for mathematical convenience and does not suggest that the apparent reaction order, c, will be the same for any salt at the same ionic strength. The apparent reaction order of **I** in Equation (4) is called c since it conveys the same information as c in Equation (2) for NaOH/NaCl solutions.

To transform the nonlinear problem into a linear problem, the logarithm of Equation (4) is taken resulting in the following relation:

$$\log k, = \log k_{OH,I} + b \log m_{OH^-} + c \log \mathrm{I} \qquad (6)$$

Regressed values of b and c are expected to be similar to those found in Sections 3.3 and **3.4,** with minor adjustments made for the inclusion of the pure NaOH and deionized water runs. Using the Powell regression technique (Kuester and Mize, 1973), b and c were calculated to be 0.57 (±0.07) and 0.26 (±0.06), respectively. Equation (4) represents the data well for m_{OH^-} from 3 x 10^{-7} to 0.01 molal and m_{Na^+} from 0 to 0.1 molal.

We would like to calculate b and c from 125° to 200°C. Unfortunately, since these data investigated the effect of added NaOH only, decoupling the effects of OH- and Na+ is difficult. The value of c has not been well characterized and no obvious trends exist as a function of temperature. For this study, c was assumed to be 0.26 over all temperatures and for m_{Na^+} less than 0.1 molal in NaOH/NaCl solutions. We can estimate b from a linear regression of the data in Figure **2,** by correlating log $[k_f / I^c]$ versus log m_{OH^-}. The resulting slopes or b values are compared to results from previous studies in Figure **5** -- note that apparent reaction orders from this study are higher than those derived from previous researchers at lower temperatures. The parameter b is not derived from an elementary reaction, therefore it is not constrained to be constant with temperature. An arbitrary fit of the data in Figure ***5*** resulted in the following correlation:

$$b = 0.694\,[1 - 0.00638\,\exp(1350 / \mathrm{T})] \qquad (\mathrm{T\ in\ K}) \qquad (7)$$

The form of this equation was chosen to model the apparent increase in b with temperature. More data is required to determine the significance of this trend.

3.5 Activation Energy for Quartz Dissolution

The activation energy for quartz dissolution in deionized water has been measured and correlated by many investigators in deionized water (Siebert *et al.*, 1963; Rimstidt and Barnes, 1980; Brady and Walther, 1990; Dove and Crerar, 1990; Bennett, 1991; and others), however, very little is known about the activation energy in other environments. In deionized water, values range from 71.3 (±10.8) kJ/ mol (Dove and Crerar, 1990) to 89 (±5) kJ/mol (Tester *et al.,* 1994). Brady and Walther (1990) found that the activation energy between 25°C and 60°C was pH dependent, being 46 kJ/mol at near-neutral pH and increasing to 54 kJ/mol at pH 8 and 96 kJ/mol at pH 11.

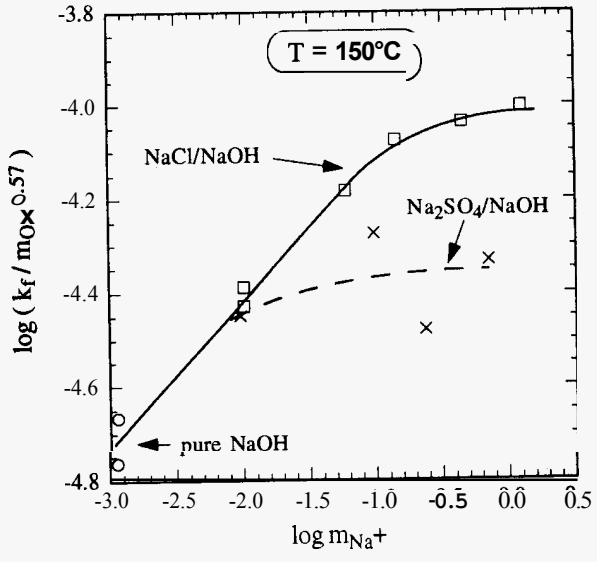

Figure 4. Quartz dissolution results showing the effect of Na+ (Na_2SO_4 versus NaCl) at constant OH- (~0.001 molal). Lines drawn to indicate trends only.

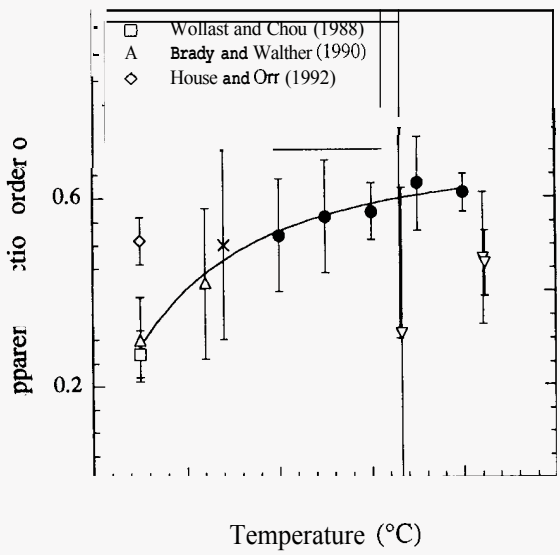

Figure 5. The apparent reaction order of OH- *(b)* as a function of temperature (line based **on** empirical fit of data using Equation **(7)** excluding Gratz and Bird **(1993)** and House and Orr (1992)).

The basis for the activation energy calculation is very important. Since at near-neutral and higher pH, quartz dissolution is base-catalyzed, the activation energy should be calculated at constant m_{OH^-} or constant pOH. All activation energies reported in this paper are apparent activation energies, since little is known about the actual elementary reactions that govern quartz dissolution. Thus, the apparent activation energy is model dependent. For example, if a model is proposed such that $k_f = k_{H_2O}\, m_{OH^-}$ in deionized water, then the apparent activation energy of k_f will be different from the apparent activation energy in k_{H_2O} since m_{OH^-} in deionized water changes with temperature.

The simplest method for calculating the apparent activation energy is to track changes in k_f at some defined set of constant conditions. This method is attractive since it involves only the overall dissolution rate and makes no assumptions about the actual rate law for quartz dissolution. Unfortunately, it does not necessarily yield meaningful values for the activation energy of quartz dissolution. However, we will employ this method as a basis for comparison with the results of previous research. Based upon the least squares regressions in Figure 2, values of k_f at log m_{OH^-} = -2.5, -4.0, and -5.5 were interpolated from 100° to 200°C and plotted on Arrhenius coordinates. The apparent activation energy (in kJ/mol) was found to be 60.1 (±12.5), 68.5 (±6.9), and 76.9 (f2.0) for log m_{OH^-} = -2.5, -4.0, and -5.5, respectively. These values support the results from Brady and Walther (1990) concerning the increase of the apparent activation energy in k_f with increasing pH, however the absolute magnitudes are higher than the Brady and Walther (1990) values.

A more appropriate analysis of the apparent activation energy for quartz dissolution calculates the temperature dependence of $k_{OH,I}$ instead of k_f, since $k_{OH,I}$ factors the effects of solution composition out of k_f. Equation (4) is used to calculate $k_{OH,I}$ for the deionized water and all of the NaOH/NaCl data except the two highest NaCl runs. The value of c is assumed to be 0.26, while b was assumed to be a function of temperature as given by Equation 7. The calculated $k_{OH,I}$ values were plotted on Arrhenius coordinates resulting in an apparent activation energy of 82.7 (f4.9) kJ/mol .

3.6 Granite Experimental Results

Two feed solutions were chosen to study the dissolution kinetics of granodiorite at 200°C; (1) deionized water (run 155), and (2) 10^{-4} molal NaOH (run 156). Two samples, 155.5 and 156.5, were sent to Los Alamos National Laboratory (LANL) to double-check our results, since our ICP analysis of sodium was questionable. The LANL results are in excellent agreement with our molybdate and ICP analyses (except Na). All of the results for runs 155 and 156 are shown in Figures 6 and 7, respectively. No results are shown for Mg and Fe since experimentally insignificant concentrations were measured (–0 molal Mg, $<10^{-6}$ molal Fe).

The surfaces of washed and reacted granodiorite samples were inspected using Scanning Electron Microscopy (SEM) to check for adhering fines and secondary precipitates. The washed granodiorite was soaked in deionized water for 30 minutes at room temperature. The reacted granodiorite was samples taken from the reactor after the two dissolution rate experiments (runs 155 and 156). The washed granodiorite had fines adhering to the surface. However, no significant population of fines is evident from SEM photographs of reacted granodiorite. A more comprehensive presentation of the granodiorite dissolution experiments including SEM photographs of washed and reacted granodiorite is given in Worley and Tester (1995b).

Calculating the dissolution rate of each phase in the granodiorite is difficult, since Si can be released from all four major phases, and Al from three of the major phases. The presence of Al in the outlet solution suggest that the dissolution of feldspars (plagioclase and microcline) are important reactions, apparently conflicting with the earlier results reported by Charles (1979). However, Charles' investigations were camed out in a recirculating system with Si concentrations approaching saturation. In these experiments, the feldspar phases are most likely to be saturated with respect to a secondary phase, thus the net observed feldspar dissolution rate is insignificant. In our experiments, the low concentrations of solution species, allows a more accurate observation of intrinsic dissolution rates.

A check on the congruency of granodiorite dissolution can be evaluated using an element balance. For example, if we assume quartz, plagioclase, and microcline dissolution are the dominant phases present, then the concentration of Al can be estimated from concentrations of Na, K, and Ca (assuming congruent dissolution).

$$m_{Al} = m_{Na} + m_K + 2\, m_{Ca} \qquad (8)$$

Using Equation **(8)** for runs 155 and 156, the estimated aluminum concentration is 286% and 58%, higher than the measured aluminum concentration, respectively. These discrepancies are

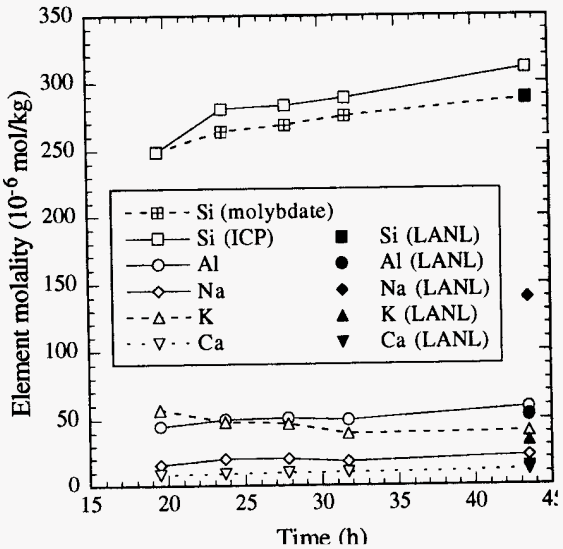

Figure 6. Composition from granite dissolution experiment with deionized water feed solution (Run 155) at 200°C as a function of time. LANL values obtained by D. Counce at Los Alamos National Laboratory (March, 1994).

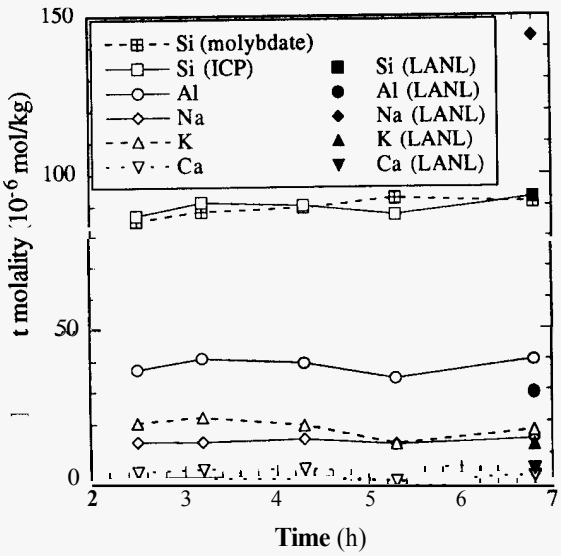

Figure 7. Composition from granite dissolution experiment with 10^{-4} molal NaOH feed solution (Run 156) at 200°C as a function of time. LANL values obtained by D. Counce at Los Alamos National Laboratory (March, 1994).

too large to be attributed to analytical uncertainty and are probably due to incongruent dissolution where the charge balancing elements (Sa. K. and Ca) dissolve more quickly than the network forming elements (Si and Al). Incongruent dissolution of feldspar surfaces has been suggested by many investigators based upon surface analytical techniques and solution compositon measurements (Chou and Wollast, 1984. 1985; Casey *et al*., 1989: Hellmann *et al*., 1990: Muir and Nesbitt. 1991: Hellmann. 1991).

Hellmann (1994) calculated albite dissolution rates based on steady state Si concentrations. Their reported steady state Al concentrations ranged from sub- to super-stoichiometric. However. they did not show Al concentrations as a function of time. so the steady state hypothesis could not be evaluated. Albite dissolution rates based on Al concentrations were significantly different than Si-based rates (up to two orders of magnitude). When dissolution rates are slower based on Al, a secondary precipitate such as boehmite [AlO(OH)] or gibbsite [$Al(OH)_3$] might be forming. Charles (1978) observed the precipitation of secondary zeolite phases on granodiorite after exposure to high temperature (approximately 300°C) circulating fluids for periods of 100 days or more.

The potential for incongruent dissolution and secondary precipitate formation makes the analysis of dissolution rate data for feldspar less straightforward than for quartz. The analysis of granodiorite (composed cf quartz, plagioclase. microcline. biotite, and other trace phases) is even more complex. In this study. our goal is not to quantitatively describe the dissolution rate of granodiorite. However, we would like to compare our results to previous granite and pure mineral (quartz and feldspar) dissolution rate experiments.

Several assumptions need to be made before the rates of each phase can be estimated. The dissolution rate of biotite is neglected due to the absence of Mg and Fe in solution. The relative importance of albite. anorthite, and microcline ($KAlSi_3O_8$) dissolution is assumed to be linearly proportional to the relative concentrations of Na, Ca. and K in solution. We recognize that secondary phase precipitation and other factors will introduce non-linearities. However. no secondary phases were observed in our experiments. With these assumptions. the amount of Al released from the congruent dissolution of each feldspar phase is estimated using the following relationships:

$$m^i_{Al} = m_{Al}\left[\frac{m_{Na}}{m_{Na} + m_K + 2\,m_{Ca}}\right] \quad (9)$$

where m^i_{Al} are the concentrations (or molality) of Al released from feldspar phase i (in mol/kg). The amount of Si released from each phase can be estimated based on the stoichiometric coefficients for Al and Si in each phase,

$$m^i_{Si} = m^i_{Al}\left[\frac{\nu^i_{Si}}{\nu^i_{Al}}\right] \quad (10)$$

where m^i_{Si} and m^i_{Al} are the concentration of Si and Al released from feldspar phase i, and ν^i_{Si} and ν^i_{Al} are the stoichiometric coefficients of Si and Al in phase i. The amount of Si released from the quartz phase can now be estimated by subtracting the sum of Si released from the feldspar phases from the total Si in solution. Dissolution rates are then calculated from the results of Equations (9) to (10) by using the following rate law assuming free dissolution conditions (no effect of precipitation on the observed dissolution rate):

$$r_i = \frac{m^i_{Si}\,F_m}{\nu^i_{Si}\,A_i} \quad (11)$$

where r_i is the net dissolution rate of phase i (mol/m^{2}s), F_m is the mass flow rate through the reactor (kg/sec), and A_i is the surface area of phase i (m^2). The surface area of phase i is calculated by multiplying the total geometric surface area by the modal analysis (vol %) of the granodiorite sample shown in Table 1. The estimated dissolution rates for each phase during runs 155 and 156 are shown in Table 2.

The results for run 155 suggest that the quartz phase does not completely dominate the production of Si in solution. We estimated log r_{qtz} = -5.8 for the quartz phase in granodiorite. Our pure quartz dissolution rates presented in earlier extrapolate to a log r_{qtz} = -6.9 accounting for OH- and ionic strength effects on the dissolution rate. However, we could not account for the potential effects of Al. Ca. and K except to include them in the ionic strength calculation. Robinson (1982) calculated the dissolution rate of granodiorite in deionized water assuming quartz is the dominant phase to be log r_{qtz} = -5.7 to -6.1 at 200°C (actual data was obtained from 194° to 208°C and adjusted to 200°C using E_A = 89 kJ/mol). Robinson (1982) did not analyze for AI so the relative importance of feldspar dissolution cannot be evaluated. If feldspar dissolution was important, the calculated quartz dissolution rates would drop. Robinson (1982) performed experiments in batch autoclave vessels. allowing the concentration of Si to rise as high as 4 x 10-3 molal. At these high concentrations. the net observed feldspar dissolution rates may be unimportant due to formation of secondary precipitates.

The results for run 156 suggest that the quartz dissolution is insignificant at 200°C using a 10^{-4} molal NaOH feed solution. This result is most likely an artifact of the assumptions used to calculate the phase dissolution rates and the uncertainties in the analytical methods. The estimated feldspar dissolution rates increased by almost an order of magnitude over the rate calculated from run 155. This trend was unexpected based on previous results for the effect of OH- on the albite dissolution rate (Hellmann, 1994). Hellmann (1994) found that the dissolution rate of albite at 200°C did not change when log m_{OH^-} was increased from -5.7 to -3.7. However. we would have expected the quartz dissolution rate increase significantly. The dissolution rate of albite on a geometric surface area basis from Hellmann (1994) was log r_{Ab} = -7.5. which is one to two orders of magnitude slower than the rates predicted from our granodiorite experiments. Hellmann (1994) compared their results with rates retrieved from Lagache (1965, 1976), who dissolved several varieties of feldspars from 100° to 200°C in a batch reactor (static autoclave). At 200°C, the log rates from Lagache's data on albite are 0.7 to 1.1 orders of magnitude lower than Hellmann's rate data. The discrepancy could be due to mass transfer limitations in the static reactor used by Lagache (1965, 1976). secondary phase precipitation, and/or uncertainties in the albite surface area.

Table 2. Estimated dissolution rates for each phase in granodiorite during runs 155 and 156 at 200°C compared to pure mineral rates under similar conditions

	log rate (mol/m^{2}s)			
	Run 155 conditions		Run 156 conditions	
	granite	mineral	granite	mineral
Quartz	-5.80	-6.9 (a)		-6.5 (a)
Albite	-6.36	-7.5 (b)	-5.58	-7.5 (b)
Anorthite	-6.65		-5.65	
Microcline	-6.76		-5.98	
Biotite	†		†	

The two granodiorite experiments conducted in this study were designed to test the ahility of our quartz dissolution model to predict the dissolution rate of the quartz phase in granodiorite. We initially thought that quartz would be the dominate phase in granodiorite dissolution based on the results of Charles (1979). However. we discovered that feldspar dissolution could not be ignored for the conditions of our study. Both the predicted quartz and feldspar dissolution rates are at least one order of magnitude higher than expected from pure mineral dissolution rates. although the quantitative nature is limited hy the assumption of embodied in Equations (8) - (11).

4. CONCLUSIONS

Quartz dissolution rates were measured from 100° to 200°C over a wide range of solution conditions. The dissolution rates in acidic HNO_3 solutions were slower than deionized water rates at the same temperature. At 175°C, the decline in dissolution rate levels off at approximately pH 3 and begins to increase again at pH 1 to 1.5. Addition of NaOH significantly enhanced the rate of quartz dissolution. The rate depended on the sodium ion concentration to the 0.26 power. while the hydroxide ion concentration dependence varied from 0.52 at 100°C to 0.62 at 200°C.

In the past. the activation energy of quartz dissolution was stated as being pH dependent (Brady and Walther. 1990). However. this is an artifact of the empirical model used in the calculation of activation energy. The concentration dependence on the rate of dissolution was separated from the temperature dependence using a fractional order empirical rate law. The apparent activation energy in the empirical rate constant was found to be 83 (±5) kJ/mol and independent of solution composition from deionized water to 0.01 molal OH- and 0.1 molal Sa+ (using NaOH and NaCl).

The applicability of the quartz dissolution kinetics to the dissolution of the quartz phase in granite was evaluated as previous studies suggested that the quartz phase would be dominant at 200°C. However, the dissolution of feldspars was found to he important as well. and may be comparable to the quartz dissolution rate depending on temperature and solution composition. The dissolution rate of individual phases in granite were estimated to be one to two orders of magnitude higher than pure mineral rates measured independently.

ACKNOU'LEDGMESTS

We gratefully acknowledge the Hot Dry Rock program at Los Alamos Sational Laboratory and the Leopold Schepp Foundation for partial support of this project. Interactions with Bruce Rohinson. Charles Grigsby, Jeffrey Feerer, Robert Charles, Dale Counce. Patricia Dove. David Duchane. James Albright, and Robert Potter were especially helpful.

REFERENCES

Armstead H.C. and J.W. Tester. (1987). Heat Mining. London. E. and F. Spon. Section 10.4.

Bennett P.C. (1991). "Quartz dissolution in organic-rich aqueous systems." *Geochim. Cosmochirn. Acto.* **55:** 1781-1797.

Brady P.V. and J.V. Walther. (1990). "Kinetics of quartz dissolution at low temperatures." *Chem. Geol.* **82:** 253-264.

Case) W.H., H.R. Westrich, G.W. Arnold and J.F. Banfield. (1989). "The surface chemistry of dissolving labradorite feldspar." *Geochim. Cosmochim. Acto.* **53:** 821-832.

Charles R.W. (1978). "Experimental Geothermal Loop: I. 295°C Study." *Los Alamos Scientific Laboratory Report LA-7334-MS.* :

Charles R.W. (1979). "Experimental Geothermal Loop: II, 200°C Study." *Los Alamos Scientific Laboratory Report LA-7735-MS.* :

Charles R.W.. C.E. Holley, J.W. Tester, C.O. Grigsby and L.A. Blatz. (1979). "Experimentally determined rock-fluid interactions applicable to a natural hot dry rock geothermal system". *TMS Paper Selection Report A80-8. The Metallurgical Society of AIME.*

Chou L. and R. Wollast. (1984). "Study of the weathering of albite at room temperature and pressure with a fluidized bed reactor." *Geochim. Cosmochim. Acta.* **48:** 2205-2217.

Chou L. and R. Wollast. (1985). "Steady-state kinetics and dissolution mechanisms of albite." *Amer. J. Sci.* **285:** 963-993.

Dove P.M. and D.A. Crerar. (1990). "Kinetics of quartz dissolution in electrolyte solutions using a hydrothermal mixed flow reactor." *Geochim. Cosmochim. Acta.* **54:** 955-969.

Gratz A.J. and P. Bird. (1993). "Quartz dissolution: Negative crystal experiments and a rate law." *Geochim. Cosmochim. Acta.* **57**: pp. 965-976.

Gratz A.J., P. Bird and G.B. Quiro. (1990). "Dissolution of quartz in aqueous basic solution, 106-236°C: Surface kinetics of "perfect" crystallographic faces." *Geochim. Cosmochim. Acta.* **54:** pp. 2911-2922.

Grigshy C.O. (1989). "Kinetics of Rock-Water Reactions".

Grigshy C.O., J.W. Tester. P.E. Trujillo and D.A. Counce. (1989). "Rock-water interactions in the Fenton Hill. Sew Mexico. hot dry rock geothermal systems I. Fluid mixing and chemical geothermometry." *Georhermics.* **18**(5/6): 629-656.

Hellmann R. (1994). "The albitz-water system: Part I. The kinetics of dissolution as a function of pH at 100. 200. and 300°C." *Geochim. Cosinochini. Acta.* **58**(2): 595-611.

Hellmann R.. C.M. Eggleston. M.F. Hochella Jr. and D.A. Crerar. (1990). "The formation of leached layers on albite surfaces during dissolution under hydrothermal conditions." *Geochim. Cosmochim. Acru.* **54:** pp. 1267-1281.

House W.A. and D.R. Orr. (1992). "Investigation of the pH dependence of the kinetics of quartz dissolution at 25°C." *J. Chem. Soc. Faraday Trans.* **8812):**233-241.

Kamiya H.. A. Ozaki and M. Imahashi. (1974). "Dissolution rate of powdered quartz in acid solution." *Geochem. J. (Japan).***8:** pp. 21-26.

Knauss K.G. and T.J. Wolery. (1988). "The dissolution kinetics of quartz as a function of pH and time at 70°C." *Geochim. Cosmochim. Acra.* **52:** pp. 43-53.

Lagache M. (1965). "Contribution a l'etude de l'alteration des feldspaths dans l'eau. entre 100 et 200°C. sous diverses pressions de CO_2, et application a la synthese des mineraux argileux." *Bull. Soc. Fr. Mineral. Cristallogr. 88:* pp. 223-253.

Lagache M. (1976). "New data on the kinetics of the dissolution of alkali feldspars at 200°C in CO_2 charged water." *Geochim. Cosmochim. Acta.* **40:** pp. 157-161.

Muir I.J. and H.W. Nesbitt. (1991). "Effects of aqueous cation on the dissolution of labradorite feldspar." *Geochim. Cosmochim. Acta.* **55**: pp. 3181-3189.

Rimstidt J.D. and H.L. Barnes. (1980). "The kinetics of silica-water reactions." *Geochirn. Cosmochim. Acta.* **44:** 1683-1699.

Robinson B.A. (1982). "Quartz Dissolution and Silica Deposition in Hot Dry Rock Geothermal Systems".

Siebert H.. W.V. Youdelis. J. Leja and E.O. Lilge. (1963). "The kinetics of the dissolution of crystalline quartz in water at high temperatures and pressures". *Unit Processes in Hydrometallurgy.* **24:** pp. 284-299.

Tester J.W.. C.E. Holley and L.A. Blatz. (1977). "Solution chemistry and scaling in hot dry rock geothermal systems". *83rd National meeting of the AIChE.*

Tester J.W., W.G. Worley. B.A. Robinson. C.O. Grigsby and J.L. Feerer. (1994). "Correlating quartz dissolution kinetics in pure water from 25 to 625°C." *Geochim. Cosmochim. Acta.* **58:** 2407-**2420.**

Wollast R. and L. Chou. (1986). "Processes. rate. and proton consumption by silicate weathering". *Trans. 13th Congr. Int. Soc. Soil.Sci.* 127-136.

Worley W.G. and J.W. Tester. (1995a). "Dissolution Kinetics and Mechanisms of Quartz from 100 to 200°C." (in prep.).

Worley W.G. and J.W. Tester. (1995b). "Dissolution Kinetics of Granite at 200°C." (in prep.).

Zemaitis J.F. Jr.. D.M. Clark, M. Rafal and N.C. Scrivner. (1986). Handbook of Aqueous Electrolvte Thermodvnamics. New York. AIChE.